Surface Holography by Angle-Resolved Electron-Energy-Loss Spectroscopy

L. S. Caputi, O. Comite, A. Amoddeo, G. Chiarello, S. Scalese, E. Colavita, and L. Papagno
Istituto Nazionale di Fisica della Materia–Unità di Cosenza and Dipartimento di Fisica, Università della Calabria, 87036 Arcavacata di Rende, Cosenza, Italy
(Received 11 March 1996)

We propose a new method to obtain surface holographic images at an atomic level by inversion of angle-resolved electron-energy-loss data. The diffraction information is contained in the intensity of a core loss peak measured in fixed directions as a function of the primary beam energy. The results obtained for the model system Ni(111)-$p(2 \times 2)$-K show that our method is valid and promising. [S0031-9007(96)00774-0]

PACS numbers: 61.14.–x, 42.40.Ht, 76.60.Dp

There is an increasing interest in developing techniques able to determine the surface structure at an atomic scale. The synchrotron radiation techniques extended x-ray absorption fine structure (EXAFS) and angle-resolved photoemission extended fine structure (ARPEFS) give structural information, respectively, in terms of a scalar radial distribution function and of a path length difference [1,2]. Real space images have been obtained by applying the holographic principle to photoelectron diffraction patterns taken at some fixed photoelectron energies over many directions in the emission emisphere [3–5]. Such methods are affected by troubles which give rise to high backgrounds, twin or streaky images.

Quite recently, a method called spatially resolved imaging of energy-dependent photoelectron diffraction (EDPD) was developed by Tong and co-workers [6,7]. In EDPD, a core level photoelectron intensity excited by an energy-scanned photon beam is measured along selected directions as scanned-energy constant-initial-state (CIS) spectra. Figure 1(a) shows a schematic diagram of the process. Photoelectrons are excited by scanned-energy photons into continuum states. The intensity of the photoelectron peak is measured in given directions as a function of the wave vector of such continuum states. Such intensity contains the diffraction information, which is extracted by Fourier inversion in real space. The CIS-EDPD method was successfully applied to the system Si(111) $(\sqrt{3} \times \sqrt{3})$-Al [8].

Few years ago, some of us developed a method, called electron-energy-loss fine structure (EELFS) [9], which gives essentially the same scalar structural information as surface EXAFS. Here we show that it is possible to obtain surface holographic images similar to those coming from CIS-EDPD, by using electrons, instead of photons, as the exciting source.

The basic ideas is sketched in Fig. 1(b). In electron-energy-loss holography (EELH), the role of the photoelectron in CIS-EDPD is played by the primary electron, which can be treated as having been emitted by the absorbing atom after the energy loss due to the excitation of a core level. Such an electron is then elastically scattered by neighbors of the absorbing atom, similar to the photoelectron in CIS-EDPD. The intensity of the loss peak taken in a given direction by scanning the primary beam energy is plotted as a function of the electron wave number. By this procedure, we obtain a constant energy loss (CEL) function, which is the direct analogy to the CIS spectrum in EDPD.

Problems arising from the use of electrons instead of photons as the exciting source should be expected in principle, and the interpretation of CEL-EELH results might be more complicated than CIS-EDPD.

The Ni(111)-$p(2 \times 2)$-K surface was selected as a model system. Using different techniques, it has been recently shown that in such phase potassium atoms are adsorbed in atop sites, at a distance of 2.9 Å from underlying nickel atoms [10–12]. Present results agree unequivocally with previous data, giving for the first time surface holograms by angle-resolved electron-energy-loss spectroscopy.

Experiments were made in a multitechnique ultrahigh vacuum system described in more detail elsewhere [13]. The Ni(111) sample was cleaned by standard procedure, and potassium was deposited using SAES Getters sources. Both the monochromator and the analyzer used for energy

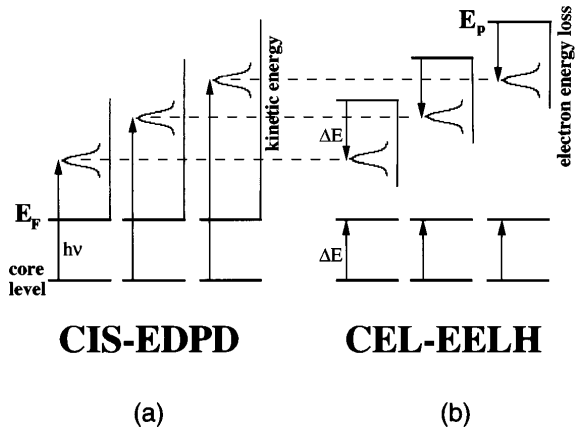

FIG. 1. Sketch of the (a) CIS-EDPD and (b) CEL-EELH processes.

loss measurements were 50 mm spherical electrostatic deflectors. The angular acceptance of the analyzer was about 2°, with a resolving power of 0.05 eV. Electron-energy-loss spectra were taken in the specular reflection mode, using a monochromatic primary beam with energy ranging from 60 eV up to 290 eV. We measured along fixed directions the intensity $I_{\hat{k}}(k)$ of the K-3p loss peak (inset of Fig. 2) as a function of the beam energy. Such potassium induced loss peak was also observed, for example, by Bugyi *et al.* [14] in their K-CO coadsorption experiments on Rh(111). Each $I_{\hat{k}}(k)$ point was an integrated K-3p peak area divided by the background area measured under the peak. The normalized CEL spectrum was obtained as $\chi_{\hat{k}}(k) = I_{\hat{k}}(k)/I_{0\hat{k}}(k) - 1$, where $I_{0\hat{k}}(k)$ is a smooth background. The wave number k of the primary electron after the energy loss is given by $k(\text{Å}^{-1}) = 0.51\sqrt{(E_P - E_L) + U_{\text{in}}}$, where E_P and E_L are the primary beam energy and the energy loss, respectively, and U_{in} is the inner potential of the Ni crystal. The electron beam energy increments were selected to give a constant wave number increment of the scattered electron, $\Delta k = 0.25$ Å^{-1}. By taking advantage of the mirror plane symmetry of the Ni(111)-$p(2 \times 2)$-K system, it was sufficient to measure CEL spectra in one-half of the emission emisphere.

Figure 2 shows a typical CEL spectrum, which exhibits an oscillating behavior with an anisotropy of about 25%. The intensity of the loss peak in a given direction is expected to be a smooth function of the primary beam energy for an isolated atom. On the other hand, diffraction of the primary electron beam is known to modulate the wave-field amplitude at the absorbing atoms [15,16]. The procedure we use to normalize the K-3p peak area is intended not only to avoid effects due to a possible drift in the primary beam current, but also to overcome primary beam diffraction problems [15]. In fact, the background of inelastically scattered electrons should follow the variations of the elastic peak intensity, which in turn are possible due to channeling effects of the primary electron beam. Thus, we interpret the modulated behavior of CEL spectra as due to the diffraction of primary electrons after their inelastic interaction with K atoms. The absence of any EXAFS-like modulation is ensured by the fact that in CEL measurements the final state of the excited core electron is always just above the Fermi level.

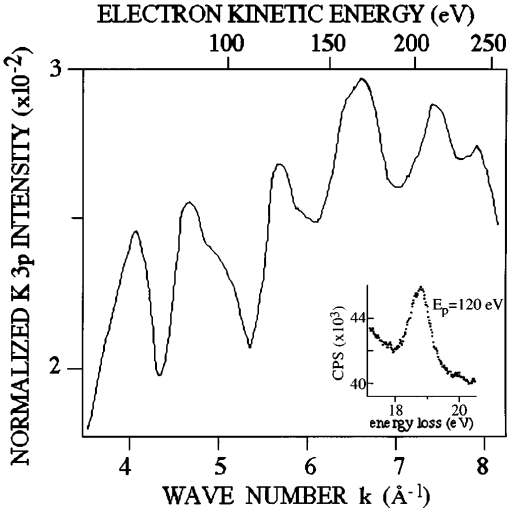

FIG. 2. A typical constant-energy-loss (CEL) spectrum measured along a fixed direction [$\phi = 0, \theta = 52°$; see Fig. 3(a)]. The inset shows the measured K-3p loss peak using a primary electron beam of energy $E_p = 120$ eV.

We elaborated CEL data using the same analysis procedure developed by Tong and Lapeyre [7,8] to invert CIS spectra. In the single scattering and small atom approximations, the normalized CIS spectrum can be written as [17]

$$\chi_{\hat{k}}(k) \propto \sum_j \left\{ F_{\hat{k}}(k, \hat{\mathbf{r}}_j) \frac{e^{ikr_j(1-\hat{\mathbf{k}}\cdot\mathbf{r}_j)}}{r_j} \right\},$$

where $F_{\hat{k}}(k, \hat{\mathbf{r}}_j)$ is an effective scattering factor which contains the photoexcitation matrix element of the absorbing atom and the elastic scattering factor of its neighboring atoms. The interference between the direct outgoing wave portion and the scattered wave portions is described by the exponential term. The transform of the CIS spectrum obtained in a given emission direction is given by

$$\psi_{\hat{k}}(\mathbf{R}) = \int_{k_{\min}}^{k_{\max}} \chi(k) e^{-ikR} e^{i\mathbf{k}\cdot\mathbf{R}} g(k)\, dk\,,$$

where $\mathbf{R}$ is the vector position relative to the absorbing atom, $k_{\min}$ and $k_{\max}$ are the integration limits of the CIS spectrum, and $g(k)$ is a window function necessary to avoid truncation effects in the Fourier transform. The inverted CIS field has maxima on surfaces defined by the condition $R(1 - \hat{\mathbf{k}} \cdot \hat{\mathbf{R}}) = r_j(1 - \hat{\mathbf{k}} \cdot \hat{\mathbf{r}}_j)$. They are parabola of revolution with axis parallel to the direction along which the CIS spectrum is measured and intersect one another only at the scatterer positions $\mathbf{R} = \mathbf{r}_j$. If the k range is large, all surfaces will be very thin and the field

$$\psi(\mathbf{R}) = \sum_{i=1}^{N} \psi_{\hat{k}_i}(\mathbf{R})$$

will give the positions of the scatterers. Here the sum is over the total number of CIS spectra. Holographic surface images are obtained by visualizing the function $u(\mathbf{R}) = |\psi(\mathbf{R})|^2$ on different planes.

Analogously, the oscillating behavior of CEL spectra would be dominated by an effective scattering factor which contains both the inelastic scattering factor of the absorbing atom and the elastic scattering factor of the scatterer. The diffraction effect is described by the same exponential term as in CIS. Then we use the same formalism to invert CEL data.

As for other electron diffraction techniques, atomic images resulting from CEL-EELH measurements are

expected to be shifted from true positions, due to the phase shift suffered by outgoing electrons when they are elastically scattered by surrounding atoms. Such a problem is even more complicated in the present case, because the dipole approximation does not hold for inelastic processes at large scattering angles, and then electrons which suffer diffraction do not have a well defined angular momentum l.

However, direct inversion of CEL data by the same procedure used for CIS-EDPD gives significative results and calls for a detailed theoretical description of the process.

We present the results of two different sets of CEL measurements. Figure 3(a) shows a sketch of the experimental geometry used, with respect to the atomic arrangement of the Ni(111)-$p(2 \times 2)$-K model system, shown in Fig. 3(b). We made a polar scan at a fixed azimuthal angle $\phi = 0$ and for θ ranging from 50° and 80° with respect to the surface normal, and an azimuthal scan, for $\theta = 52°$ and ϕ ranging from $-20°$ to 20° with respect to the $[0\bar{1}1]$ azimuthal direction. The holographic functions $u_\theta(\mathbf{R})$ and $u_\phi(\mathbf{R})$ were obtained from a total of 6 and 9 CEL curves for the polar and azimuthal scans, respectively. Figure 4(a) shows a gray-scale image of a cut of the $u_\theta(\mathbf{R})$ function along the $(0\bar{1}1)$ plane which contains the absorbing potassium atom, whose position is indicated by a star. In such a polar scan image, good resolution is expected in the $(\bar{2}11)$ plane, which is the fixed scattering plane in the polar scan [7]. In fact, the image in Fig. 4(a) shows good resolution in the [111] direction [which belongs to the $(\bar{2}11)$ plane], and bad resolution in the $[\bar{2}11]$ direction. We attribute the image in Fig. 4(a) as due to Ni atom 1 in our model system, on top of which the K atom is bonded. The position of such an Ni atom is shown in Fig. 4(a) by a circle, at a distance of 2.9 Å from K atom, as deduced from literature data [10–12]. The image obtained is shifted by about 0.7 Å, very likely to phase shift effects.

Such experimental observation induced us to cut the $u_\phi(\mathbf{R})$ function, obtained from the azimuthal scan, along a (111) plane located 2.2 Å below K atom. The resulting image is shown in Fig. 4(b), where circles represent surface Ni atoms of the model system, labeled as in

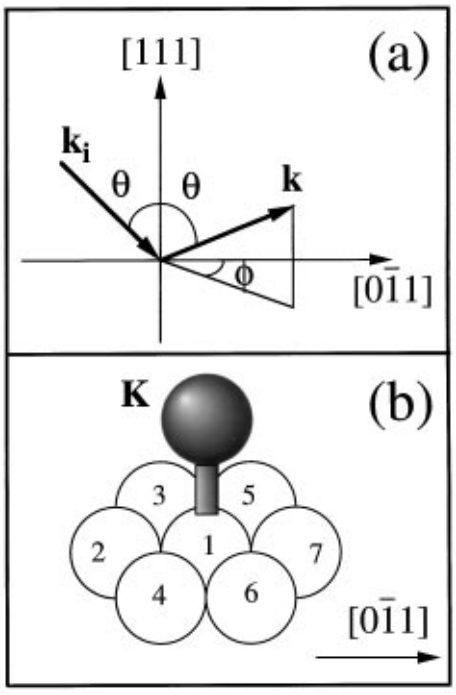

FIG. 3. (a) Experimental geometry used for CEL measurements; (b) atomic arrangement of the Ni(111)-$p(2 \times 2)$-K model system, with numbers labeling Ni atoms as labeled on the images.

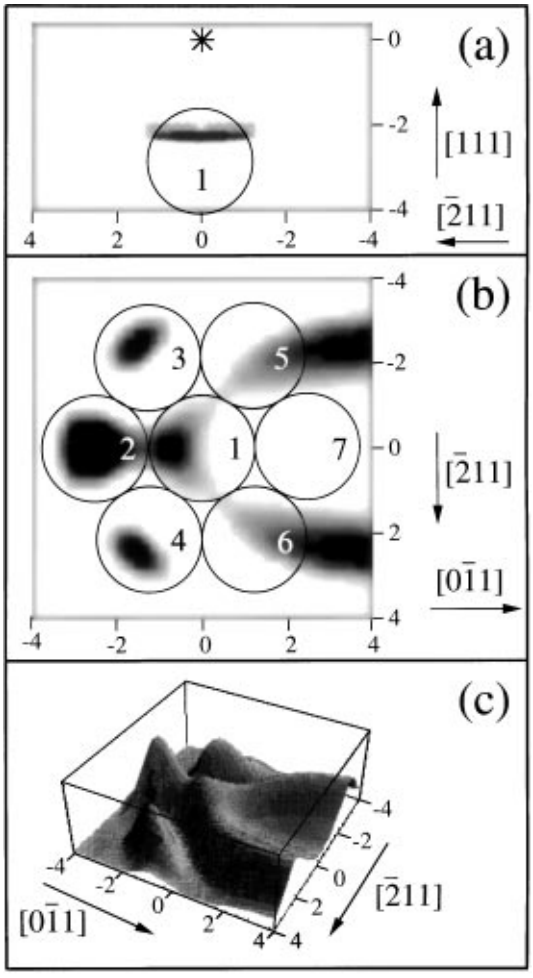

FIG. 4. (a) Gray-scale image of a cut of the experimental $u_\theta(\mathbf{R})$ function along a $(0\bar{1}0)$ plane containing the absorbing K atom, whose position is indicated by a star; the circle represents the position of Ni atom 1 of the model system, at a distance of 2.9 Å from K atom. (b) Gray-scale image of a cut of $u_\phi(\mathbf{R})$ along a (111) plane located 22 Å below the K atom; circles show the position of surface Ni atoms, labeled as in Fig. 3(b). The image in (b) is also shown in (c) by indicating the $u_\phi(\mathbf{R})$ function along an axis perpendicular to the image plane.

Fig. 3(b). The same image is shown in Fig. 4(c), in which the $u_\phi(\mathbf{R})$ function is indicated on an axis perpendicular to the image plane.

The best result is obtained for the position of atom 2, which is located just behind the absorbing K atom, with respect to the analyzer. Thus, as in CIS-EDPD, the best results are obtained when the outcoming electron wave is backscattered by a neighboring atom towards the analyzer. When other atoms are considered, their position is reproduced worse and worse higher is the distance from the backscattering position of atom 2. Atoms 3 and 4 still give a good signal, although shifted from the correct position. Such shift is higher for atom 1, and, on going far from the backscattering direction, atoms 5 and 6 just give rise to a shifted and elongated image. The contribution from atom 7 is negligible.

Thus, although in our treatment of experimental data we disregard any effect due to the use of electrons as the exciting probe, the results give evidence that the CEL-EELH method is able to give holographic images of surface structures. The diffraction mechanism should be very similar to the CIS-EDPD mechanism, as shown also by the evidence that our images give good results only for atoms located in a cone where the electron wave is backscattered toward the analyzer. The artifacts contained in the EELH images can be eliminated by a proper theoretical description which eventually could introduce some modifications in the inversion procedure. Moreover, relevant directions in the emission emisphere could be determined from a first broad scan, and then neighboring atoms could be located by taking CEL spectra in cones with axes parallel to those directions.

In conclusion, we have shown that, in spite of the complexity of the electron-atom interaction governing the electron-energy-loss process, treating electron-energy-loss results, taken in the CEL mode, by the same procedure adopted for synchrotron radiation CIS results, we obtain significative and encouraging results. In fact, our results show that the CEL-EELH method is able to give structural information in terms of surface holograms. They are chemically specific of the absorbing atom and allow us to locate its nearest neighbor atoms with an accuracy similar to CIS-EDPD.

[1] L. Q. Wang, A. E. Schach von Wittenau, Z. G. Ji, L. S. Wang, Z. Q. Huang, and D. A. Shirley, Phys. Rev. B **44**, 1292 (1991).

[2] J. J. Barton, C. C. Bahr, Z. Hussain, S. W. Robey, J. G. Tobin, L. E. Klebanoff, and D. A. Shirley, Phys. Rev. Lett. **51**, 272 (1983).

[3] J. J. Barton, Phys. Rev. Lett. **61**, 1356 (1988).

[4] G. K. Harp, D. K. Saldin, and B. P. Tonner, Phys. Rev. Lett. **65**, 1012 (1990).

[5] G. S. Herman, S. Thevuthasan, T. T. Tran, Y. J. Kim, and C. S. Fadley, Phys. Rev. Lett. **68**, 650 (1992).

[6] S. Y. Tong, Hua Li, and H. Huang, Phys. Rev. Lett. **67**, 3102 (1991).

[7] S. Y. Tong, H. Huang, and C. M. Wei, Phys. Rev. B **46**, 2452 (1992).

[8] H. Wu, G. J. Lapeyre, H. Huang, and S. Y. Tong, Phys. Rev. Lett. **71**, 251 (1993).

[9] L. Papagno, M. De Crescenzi, G. Chiarello, E. Colavita, R. Scarmozzino, L. S. Caputi, and R. Rosei, Surf. Sci. **117**, 515 (1982).

[10] D. L. Alder, I. R. Collins, X. Liang, S. J. Murray, G. S. Leatherman, K. D. Tsuei, E. E. Chaban, S. Chandavarkar, R. McGrath, R. D. Diehl, and P. H. Citrin, Phys. Rev. B **48**, 17 445 (1993).

[11] D. Fisher, S. Chandavarkar, I. R. Collins, R. D. Diehl, P. Kaukasoina, and M. Lindroos, Phys. Rev. Lett. **68**, 2786 (1992).

[12] Z. Q. Huang, L. Q. Wang, A. E. Schach von Wittenay, Z. Hussain, and D. A. Shirley, Phys. Rev. B **47**, 13 626 (1993).

[13] L. S. Caputi, G. Chiarello, S. Molinaro, A. Amoddeo, and E. Colavita, J. Electron Spectrosc. Relat. Phenom. **64/65**, 145 (1993).

[14] L. Bugyi, J. Kiss, K. Révész, and F. Solymosi, Surf. Sci. **233**, 1 (1990).

[15] S. A. Chambers, Surf. Sci. Rep. **16**, 261 (1992).

[16] S. Valeri, A. di Bona, and G. C. Gazzadi, Surf. Sci. **311**, 422 (1994).

[17] S. Y. Tong, C. M. Wei, T. C. Zhao, H. Huang, and Hua Li, Phys. Rev. Lett. **66**, 60 (1991).